M. Stiftinger / S. Selberherr

A Physically Based Analytical Model for Vertical DMOS Transistors

Abstract

An approach for a physically based analytical DC– and AC–model for vertical DMOS (double-diffused MOS) transistors is presented. It accounts for non-uniform channel doping concentration in lateral direction, for space-charge limited current in the drift region and is able to describe the behavior of the device without kinks and glitches in the device characteristics. Our model is supported by two-dimensional numerical device simulations.

1   Introduction

Smart Power MOS transistors serve primarily as an interface between digital control logic and the power load. Since they are also used in analog applications there are high demands on the accuracy of analytical models for circuit simulation.

Numerical device simulations are an important prerequisite for the development of a physically based analytical device model. Extensive simulations with MINIMOS [5] and BAMBI [2] provided insight in the physically important effects for the DMOS transistor.

Vertical DMOS transistors can consist of a large number of DMOS cells (e.g. up to 10.000) which have a common drain, a burried layer which is contacted to the surface by one or more very deep implants. Figure 1 shows the structure of a vertical DMOS transistor. The current flows through the channel in lateral direction into the drift region and then in vertical direction to the drain burried layer. The drift region is lowly n–doped so that there is the major voltage drop between source and drain. Therefore the drift region represents a considerable resistance (which is voltage dependent as will be shown later).

2   The model

The results by the numerical simulations have led us to a first subcircuit approach which is shown in Figure 2. The channel is represented by an enhanced analog MOSFET model. The drift region is approximated by a modified JFET model, the gate–drain capacitance is modeled by a nonlinear capacitance which also accounts for the part of the drift region which has a common interface with the gate oxide. The parasitic behavior under reverse bias is described by standard bipolar transistor models.

Starting from this subcircuit models for the devices have been developed that account for the specific situation in the vertical DMOS. In the following the most important two devices, the modified JFET and the enhanced MOSFET model are discussed.

2.1   The modified JFET model

It can easily be seen that in dependence from the voltage between source and drain of the DMOS there is a space charge region between the p–body and the n–drift region. Therefore the area where the current can flow from the interface between drift region and gate oxide to the drain burried layer is voltage dependent. Numerical device simulations with BAMBI have shown that the space charge region which grows in lateral and vertical direction with increasing source–drain voltage limits the current flow in the drift region. Basic considerations show that this behavior can be modeled analogously to the standard analytical JFET description with the exception of the special geometry of the DMOS cell. A simple model is given in [7]. Figure 3 shows the relevant geometry. The pinch–off voltage can be calculated as follows (U_{bi} is the built–in potential):

$$U_p = U_{bi} - \frac{q N_{epi} \left(L_p - 2 x_{body} \right)^2}{8 \epsilon_S} \tag{1}$$

The DMOS JFET current can be given (under consideration of the drift velocity saturation) by:

$$I_D = \frac{A_d q N_{epi} \mu_{epi}}{x_d \left(U_{bi} - U_p \right)} \cdot \frac{\left(U_{BD} - U_p - \frac{1}{2} U_{dD} \right) U_{dD}}{\left(1 + \left(\frac{U_{dD} \mu_s}{x_d v_{max}} \right)^a \right)^{1/a}} \tag{2}$$

For μ_s the perpendicular field reduction of the mobility in the epi–layer is already taken into account, x_d is the vertical extent of the space charge region which can also easily be calculated. A_d is the maximal area for the vertical current flow. The U_{dD} denotes the voltage between nodes 22 and 11 in Figure 2.

2.2 The enhanced MOSFET model

Both measurements and numerical device simulation indicate that especially in the AC–case the strongly non-uniform channel doping in the lateral direction has important influence on the device behavior. Therefore a "classical" analog MOS model [1] has been enhanced to account for those effects. Numerical device simulations show that for a non-uniform channel doping in lateral direction the drain current becomes greater than for a "classical" uniform doping in the direction of current flow in the channel (Figure 4). Figure 5 shows results of numerical device simulations for varying channel length. The doping concentrations on both ends of the channel were fixed at values which differed at about one order of magnitude. For shorter channel lengths the channel doping profile becomes "steeper" and vice versa. The results of these simulations for e.g. C_{gsb} indicate that there is a dependence on the "steepness" of the channel doping profile. The channel doping profile of the n–channel vertical DMOS transistor is defined by the different lateral diffusions of p–base and n$^+$–source. We approximate this by an exponential shape:

$$N_A(x) = N_A(0) \exp\left(-\eta\frac{x}{L}\right) = N_{A0} \exp\left(-\eta\frac{x}{L}\right) \tag{3}$$

Most of the literature concerned with modeling of Smart Power devices deals with the drift region. In most cases the non-uniform channel doping is neglected. The first approach in our model was according to one of the few that have been published ([3]).

2.2.1 The model according to Kim and Fossum

Starting point is the drain current in the strong inversion regime:

$$I_D = -W\mu_{eff}E_x(x)q_C(x) = -W\mu_{eff}q_C(x)\frac{dU_C}{dx} \tag{4}$$

$E_x(x)$ is the electric field in lateral direction, the channel and the bulk charge density are given by:

$$q_C = -C_{ox}\left(U_{GB} - U_{FB} - 2\Phi_F - U_{CB}\right) - q_B \tag{5}$$

$$q_B = -C_{ox}\left(\gamma f_c\sqrt{2\Phi_F - U_{BS}} + \kappa f_B\left(U_{CB} + U_{BS}\right)\right) \tag{6}$$

with:

$$\Phi_F = U_T \ln\frac{N_A}{n_i} \tag{7}$$

$$\gamma = \frac{\sqrt{2\epsilon_S q N_A}}{C_{ox}} \tag{8}$$

$$f_B = \frac{\gamma f_c}{2\sqrt{2\Phi_F - U_{BS}}} \tag{9}$$

In this approach equation 4 is integrated neglecting the dependency of q_C on $N_A(x)$. As result the "classical" solution is obtained:

$$I_D = \frac{W}{2L_{eff}}\mu_{eff}\left(2C_{ox}U_{GSeff} - \left(C_{ox} + C_{dB}\right)U_{DSeff}\right)U_{DSeff} \tag{10}$$

The quantity C_{dB} can be regarded as derivative of the bulk depletion charge with respect to the channel potential and is given in the case of a uniform channel doping by:

$$C_{dB}^{classical} = \kappa f_B \tag{11}$$

Kim and Fossum now calculate C_{dB} taking into account the non-uniform channel doping. To able to do this analytically the following assumptions are made: The channel potential varies linearly between source and drain ($U_{CB}(x) \approx U_{DSeff}\frac{x}{L_{eff}}$) and $C_{dB} \neq f(x)$. Furthermore the dependence of Φ_F from $N_A(x)$ is neglected, which can safely be done, because Φ_F depends only logarithmically on $N_A(x)$. Also the assumption of the linear variation of the channel potential is tolerable. Due to fact that the doping concentration on the source side of the channel is much higher than on the drain side the electric field on

the source end of the channel is higher than on the drain side. Therefore the electrons reach the saturation velocity first on the source side with increasing source drain voltage and move with that velocity across the channel. Therefore this device shows no pinch–off behavior in the classical sense.

Making no additional simplifications (in contrast to [3]) there are two additional terms in the resulting formula for the drain current. The factor C_{B1} is proportional U_{DSeff}^2 in the drain current formula, Q_{B2} is proportional U_{DSeff} and therefore has the dimension of a charge:

$$C_{B1} = C_{ox}\kappa f_{B0}\frac{\eta}{2}\frac{1}{\exp\left(\frac{\eta}{2}\right)-1}\left(1-\frac{\eta}{4}\right) \tag{12}$$

$$Q_{B2} = -C_{ox}\kappa f_{B0}\frac{\eta}{2}\frac{1}{\exp\left(\frac{\eta}{2}\right)-1}\frac{1}{\kappa}\left(2\Phi_F - U_{BS}\left(1-\frac{\kappa}{2}\right)\right) \tag{13}$$

with

$$f_{B0} = \sqrt{\frac{\epsilon_s q N_{A0}}{2\left(2\Phi_F - U_{BS}\right)}}\frac{f_c}{C_{ox}} \tag{14}$$

For $\eta \to 0$ the classical solution is obtained. Both terms lead to an increase of the drain current. This is the expected result due to a higher channel conductivity because of a smaller depletion charge at the drain end of the channel. But the dependency of C_{B1} and Q_{B2} on η shows maxima which can hardly be physically explained (see Figure 6). The second major drawback of this approach is that it is not obvious how it can be generalized for a charge based capacity model.

2.2.2 The new DC–model

Because of the shortcomings of the above approach a new model has been developed. The dependence of q_C on $N_A(x)$ in the integration of equation 4 is no longer neglected. The equation to be integrated reads:

$$\int_0^{L_{eff}} I_{DD}\,dx = \int_0^{L_{eff}} W\mu_{eff}C_{ox}\left(U_{GS} - U_{FB} - 2\Phi_F - U_{DSeff}\frac{x}{L_{eff}} - \right. \tag{15}$$

$$\left. -f_{B0}\exp\left(-\frac{\eta}{2}\frac{x}{L_{eff}}\right)\left(2\left(2\Phi_F - U_{BS}\right)+\kappa U_{DSeff}\frac{x}{L_{eff}}\right)\right)\frac{U_{DSeff}}{L_{eff}}\,dx$$

This can be done under the assumption of a linearly distributed channel potential. The dependence of Φ_F on is again neglected.

Both the calculation and the results are simpler than in the above case. In addition the result is more physically sound. It reads:

$$I_D = \frac{W}{L_{eff}}\mu_{eff}C_{ox}\left(U_{GS} - U_{FB} - 2\Phi_F + 2f_{B0}\left(2\Phi_F - U_{BS}\right)\frac{2}{\eta}\left(\exp\left(-\frac{\eta}{2}\right)-1\right) - \right.$$

$$\left. -U_{DSeff}\left(\frac{1}{2} - f_{B0}\kappa\left(\left(\frac{2}{\eta}\right)^2\left(\exp\left(-\frac{\eta}{2}\right)-1\right)+\frac{2}{\eta}\exp\left(-\frac{\eta}{2}\right)\right)\right)\right)U_{DSeff} \tag{16}$$

For $\eta = 0$ the classical result is obtained. The additional terms are shown in Figure 7. The term that is linearly dependent on U_{DSeff} modifies U_{GSeff} in our implementation. This has the advantage that the exponential dependence of I_D on U_{GS} in the weak inversion regime which is modeled continously by U_{GSeff} is not altered by the additional terms. Both terms show an expected dependence on η and also lead to a higher drain current. Figure 8 shows the effect of η in the new analytical model.

Another important advantage of this approach is that it can be generalized to a charge based capacitance model which is shown in the next section.

2.2.3 An enhanced charge based capacitance model

A charge based capacity model guarantees conservation of charge, which can be important for circuit simulations. Therefore the starting point of our enhanced capacity model is the model by Oh, Ward, and Dutton [4]. It calculates the charges which are assigned to the four MOS terminals from which the capacitances can be determined as derivatives with respect to the terminal voltages. The problem in the

charge based method is the separation of the channel charge in the drain and the source charges. These charges read in above model:

$$Q_D = -qW \int_0^L n(x,t)\frac{x}{L}dx \tag{17}$$

$$Q_S = -qW \int_0^L n(x,t)\left(1-\frac{x}{L}\right)dx \tag{18}$$

In order to be able to perform the integration the following equations which can be derived from the basic relation $I_D = -Wqn(x)\mu\frac{dU_C}{dx}$ are used:

$$I_D = -\frac{W}{L} \int_0^{U_{DS}} qn(U_C)\mu dU_C \tag{19}$$

$$dx = -\frac{Wqn(U_C)\mu}{I_D}dU_C \tag{20}$$

$$x = -\frac{W \int_0^{U_C(x)} qn(U_C)\mu dU_C}{I_D} \tag{21}$$

The drain charge e. g. reads:

$$Q_D = -WL\frac{\int_0^{U_{DS}} q^2n^2(U_C)\int_0^{U_C} qn(U_{C\prime})dU_{C\prime}dU_C}{\left(\int_0^{U_{DS}} qn(U_C)dU_C\right)^2} \tag{22}$$

In the classical case the channel charge density is given by:

$$q_C(U_C) = C_{ox}(U_{GSeff} - (1+\kappa f_B)U_C) \tag{23}$$

For the case of a non-uniform channel doping the following relationship can be used instead:

$$q_C(U_C) = C_{ox}\left(U_{GS} - U_{FB} - 2\Phi_F - U_C(x) - f_{B0}\exp\left(-\frac{\eta}{2}\frac{x}{L}\right)(2(2\Phi_F - U_{BS}) + \kappa U_C(x))\right) \tag{24}$$

The integrations in equation 22 can again be performed under the assumption of a linearly distributed channel potential. It can easily be seen that for $\eta \rightarrow 0$ the classical result is obtained. Results and comparisons of numerical device simulations and the enhanced analytical capacity model will be presented at the conference.
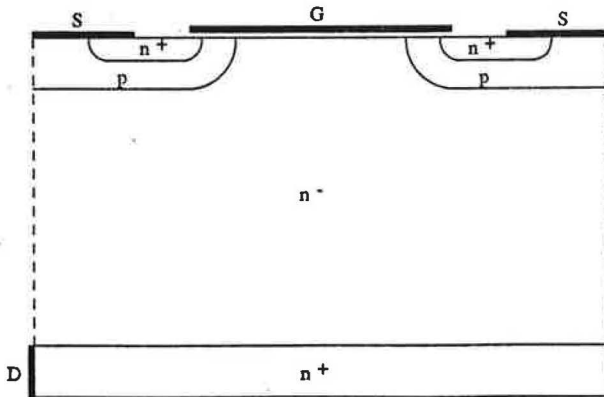

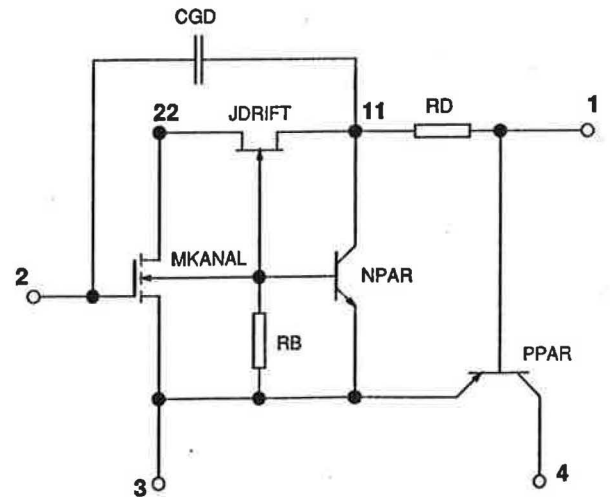Fig.1. Structure of the vertical DMOS transistor

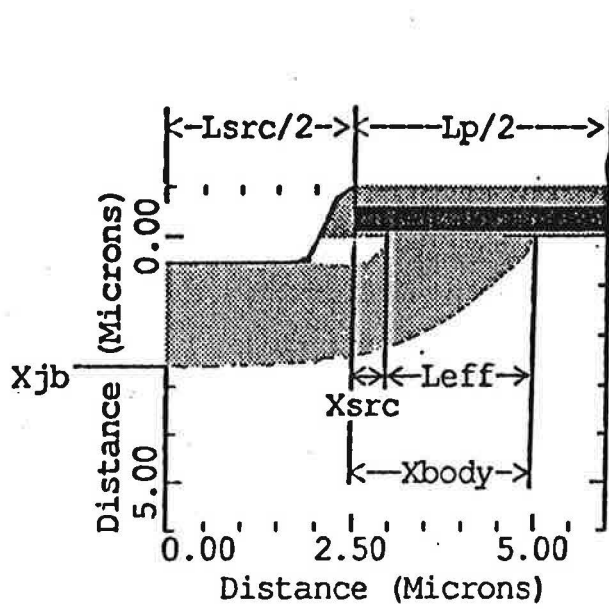Fig.2. Subcircuit model for the vertical DMOS transistor

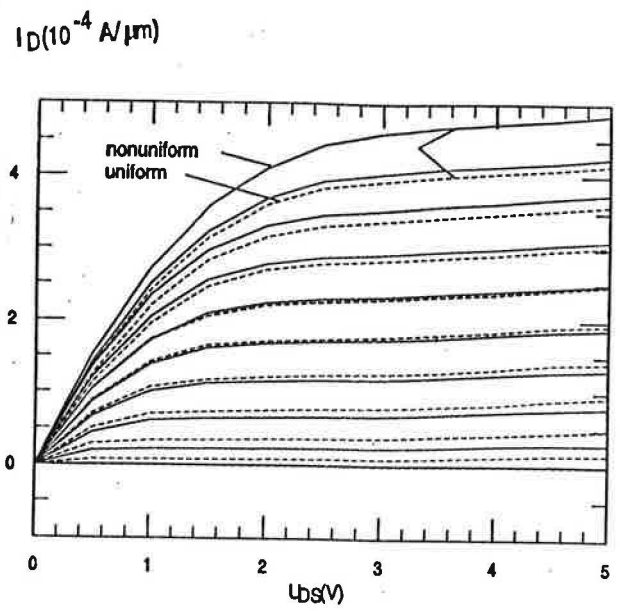Fig.3. Geometry of the DMOS cell for the modified JFET model

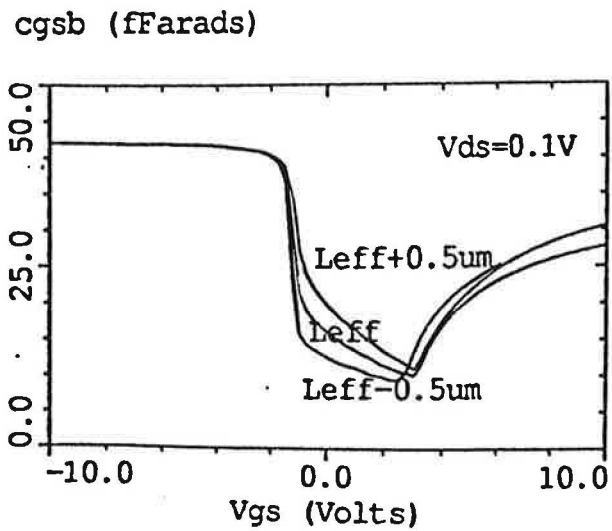Fig.4. MINIMOS simulations of a MOSFET with uniform and non-uniform channel doping

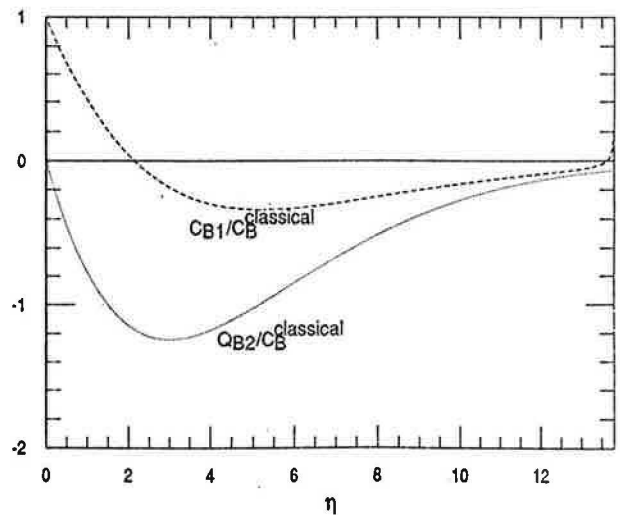
Fig.5. Numerical simulation of C_{gsb}
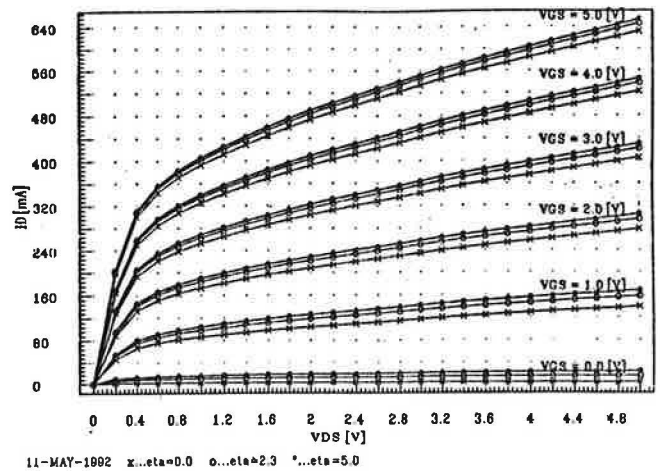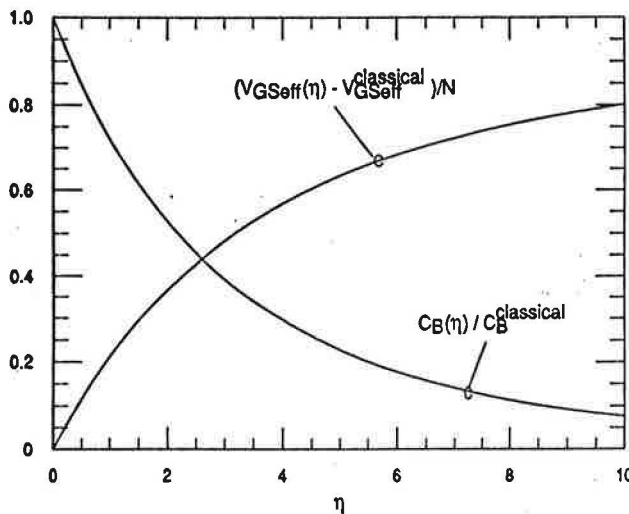

Fig.6. C_{B1} and Q_{B2} over η

Fig.7. $U_{GSeff}(\eta) - U_{GSeff}^{classical} / \left(2\frac{C_{dB}^{classical}}{C_{ox}}(2\Phi_F - U_{BS})\right)$ and $C_{dB}(\eta)/C_{dB}^{classical}$ over η

Fig.8. The effect of η in the enhanced MOSFET model for nonuniform channel doping

Acknowledgement

References

[1] U. Claeßen, G.E. Müller-L., B. Lemaître, H.L. Zapf, "Erhöhte Genauigkeit bei der Simulation analoger CMOS-Schaltungen durch ein verbessertes MOS-Kompaktmodell", *AEÜ*, Vol. 44, No. 2, pp. 139–147, 1990.

[2] A.F. Franz, G.A. Franz, W. Kausel, G. Nanz, P. Dickinger, C. Fischer, "BAMBI 2.1 User's Guide", *Technical University Vienna*, 1989.

[3] Y.-K. Kim, J.G. Fossum, "Physical DMOST Modeling for High-Voltage IC CAD", *IEEE Trans.Electron Devices*, Vol. 37, No. 3, pp. 797–803, March 1990.

[4] S. Oh, D.E. Ward, R.W. Dutton "Transient Analysis of MOS Transistors", *IEEE J. Solid State Circuits*, Vol. SC-15, No. 4, pp. 636–643, August 1980.

[5] S. Selberherr, P. Habaš, O. Heinreichsberger, Ph. Lindorfer, P. Pichler, H. Pötzl, A. Schütz, M. Stiftinger, M. Thurner "MINIMOS 5 User's Guide", *Technical University Vienna*, 1990.

[6] W. Soppa, "Stand der Modellierung von Vertikal-DMOSFET's in Smart-Power-Mischtechnologie", *Internal Rep., SIEMENS HL CAD 31*, München, September 1990.

[7] W. Soppa, J. Hänseler "A Process Oriented VDMOSFET Model for Circuit Simulation", *Proceedings of ISPSD'92*, Tokyo, Japan, May 1992.

Authors:
Dipl.-Ing. Stiftinger, Martin
Univ. Prof. Dipl.-Ing. Dr. techn. Selberherr, Siegfried
Institute for Microelectronics, Technical University Vienna, Gußhausstraße 27–29
A-1040 Wien, AUSTRIA